PHYSICAL REVIEW B **73**, 075302 (2006)

Adsorption of Sb_4 on Ge(001) and Si(001) surfaces: Scanning tunneling microscopy and first-principles calculations

E. Martínez-Guerra
Centro de Investigación Científica y de Educación Superior de Ensenada, Apartado Postal 2681, Ensenada, Baja California 22800, Mexico

G. Falkenberg and R. L. Johnson
Institut für Experimentalphysik, Universität Hamburg, Luruper Chaussee 149, D-22761 Hamburg, Germany

Noboru Takeuchi
Centro de Ciencias de la Materia Condensada, Universidad Nacional Autónoma de México, Apartado Postal 2681, Ensenada, Baja California 22800, Mexico

(Received 15 September 2005; published 1 February 2006)

We have performed first-principles total energy calculations and scanning tunneling microscopy experiments to study the energetics and the atomic structures resulting from the adsorption of Sb_4 molecules on the Ge and Si(001)-$c(2\times4)$ surfaces. Several metastable arrangements are found: Sb_4 molecules can adsorb as three-dimensional clusters or as flat tetramers. The latter are more stable and can reside either centered on top of the Ge dimer row or half on-top and half over the trench between dimer rows, and in the trenches between two dimer rows. It is found that it is energetically more favorable for Sb_4 to split into two Sb_2 dimers adsorbed parallel and on top of the Ge (Si) dimer rows. Simulated scanning tunneling microscopy images are in excellent agreement with the experimental data. The energetics of the diffusion of the dimers into the first Ge (Si) layer is also discussed.

DOI: 10.1103/PhysRevB.73.075302 PACS number(s): 68.35.−p, 68.37.Ef, 71.15.−m

I. INTRODUCTION

The study of the adsorption of group V metals, such as As, Sb, and Bi, on Si and Ge surfaces is of technological importance because of their use as surfactants in the epitaxial growth of Ge on Si and Si on Ge substrates.[1,2] This has motivated theoretical and experimental studies of the growth of group V metals on Si(001)[3–8] and Ge(001) surfaces.[8–12]

The interaction of Sb with Si and Ge(001) surfaces have been studied using a number of experimental techniques including x-ray and ultraviolet photoelectron spectroscopy,[9,12–15] surface x-ray diffraction,[11] low-energy electron diffraction (LEED),[13,16,17] high-energy electron diffraction,[9,13] scanning tunneling microscopy (STM),[3,16–23] scanning tunneling spectroscopy (STS),[19,24] and ion channeling.[25] Most experiments were performed on samples with one Sb monolayer coverage. Deposition of Sb multilayers followed by annealing at elevated temperatures produces a surface with (2×1) periodicity by breaking all of the Si (Ge) surface dimers and the formation of a layer of Sb dimers.

Although the behavior of Sb on Si and Ge(001) is well understood in the full monolayer regime, this is not the case at low coverages. There are only a few studies of the initial stages of adsorption of Sb on Ge Refs. 16 and 26 or Si(001).[20–22,27] Dixon and coworkers have studied the structure and stability of Si(001) with submonolayer coverages of Sb, and found an ordered $c(4\times4)$-Sb reconstruction between 0.2 and 0.3 monolayers (ML).[27] STM experiments have shown that Sb_4 molecules can be adsorbed on Ge(001) surfaces as two- and three-dimensional (3D) clusters, or as two Sb dimers. Sb dimers have a tendency to diffuse into the Ge substrate after annealing. Currently information about the energetics of these systems and the structural properties is lacking. In this paper, we investigate the adsorption of Sb_2 and Sb_4 on the Ge(001)-$c(2\times4)$ and Si(001)-$c(2\times4)$ surfaces. We report total energy calculations of different molecular configurations to identify which structures can exist in the initial stages of adsorption. Simulated scanning tunneling microscopy (STM) images are compared with experimental STM data. We have also studied the diffusion of the dimers into the first layer. Similar calculations were performed for Sb on Si(001), with slightly different results.

II. METHOD

A. Experimental

The experiments were performed in an ultrahigh vacuum (UHV) system with a base pressure less than 4×10^{-11} mbars. The UHV system is equipped with STM, LEED, and reflection high-energy electron diffraction (RHEED). Polished (001) wafers ($\sim7\times4\times0.5$ mm^3) were rinsed in pure methanol, loaded in the UHV chamber and outgassed by dc heating at temperatures up to 650 °C. Clean reconstructed (001) surfaces were prepared by repeated cycles of sputtering with 500 eV Ar$^+$ ions at a temperature of 500 °C and annealing at 650 °C, until a sharp (2×1) LEED pattern with a low background and modulated streaks indicating extended $c(4\times2)$ domains were observed. Sb was evaporated from an effusion cell with a pyrolitic boron nitride (PBN) crucible at a rate of $\sim5\times10^{-4}$ MLs, where one

1098-0121/2006/73(7)/075302(8)/$23.00

monolayer (1 ML) is equal to 6.24×10^{14} atoms cm^{-2}. The effusion cell has been calibrated with a quartz microbalance and by counting the antimony atom density observed in STM. Above 670 K the temperature was measured with an optical pyrometer.

B. Theoretical method

Our calculations are performed within the *ab initio* molecular dynamics (MDs) approach,[28] which allows the Kohn-Sham equations of the local density functional theory[29,30] to be solved in a very efficient way.

We have used a repeated slab configuration, with five layers of Ge (Si) atoms and Sb atoms on top of the first layer. Each layer had 16 Ge (Si) atoms and $p(4\times4)$ periodicity. Neighboring slabs were separated by 9 Å empty space and the dangling bonds of the lowest Si layer were saturated by a layer of 32 hydrogen atoms. We fixed the positions of the atoms in the two lowest layers to simulate a bulklike termination. The topmost four Si layers and the Sb atoms were allowed to move freely. The effect of the number of layers, vacuum size, and number of atoms/layer (**k**—point sampling) has been tested previously for Sb/Ge(001) and Sb/Si/Ge(001).[7,31] A kinetic energy cutoff of 10 Ry was used and only the Γ point of the surface supercell Brillouin zone was sampled because of the large size of the unit cell. We have used *ab initio* norm-conserving pseudopotentials for Ge, Si, and Sb. They included s and p nonlocal terms, and were treated within the Kleinman-Bylander scheme.[32] The Ge, Si, and Sb pseudopotentials have been tested in previous studies on the adsorption of one monolayer of Sb on Si(111),[33] Sb on Si(001),[31] Sb on Ge(111),[34] and Sb on Ge(001).[7] A steepest descent (SD) algorithm was used for electronic minimization at fixed ionic position. This was combined with a similar steepest descent (SD) dynamics for the ions to determine the optimum surface structure.

III. RESULTS

Figures 1(a) and 1(b) are STM images characteristic for Ge(001) surfaces after deposition of 0.1 ML Sb (i.e., 0.025 ML Sb_4) at room temperature [Fig. 1(a)] and after annealing at 690 K [Fig. 1(b)]. Besides the undisturbed dimer rows of the clean Ge(001) surface, four types of protrusions can be distinguished in Fig. 1(a): square-shaped protrusions located at two different positions relative to the Ge lattice ("A," "B"), oval-shaped protrusions ("C"), and ball-shaped protrusion ("D"). A simple mapping of the positions of the square-shaped protrusions to atomic positions indicates that this feature is made up of two dimers. The Sb dimers are oriented perpendicular to the Ge dimers of the substrate. One of the dimers of protrusion "A" is located close to a bridge position and the other close to a cave position of the Ge substrate. However, both dimers of protrusion "B" are positioned close to "on top" positions. The apparent height of the protrusions above the Ge dimer rows is 1.4 Å for protrusion type "A" and 1.8 Å for protrusion type "B." The tendency to coalesce into chains oriented perpendicular to the Ge dimer rows is observed to increase with coverage. The oval- and ball-shaped protrusions are located on top of the Ge dimer rows and the oval-shaped protrusions are elongated along the Ge dimer rows. The corrugation above the Ge dimer rows is 2.5 Å for the oval-shaped protrusions and 3 Å for the round-shaped protrusions under the specified tunneling conditions.

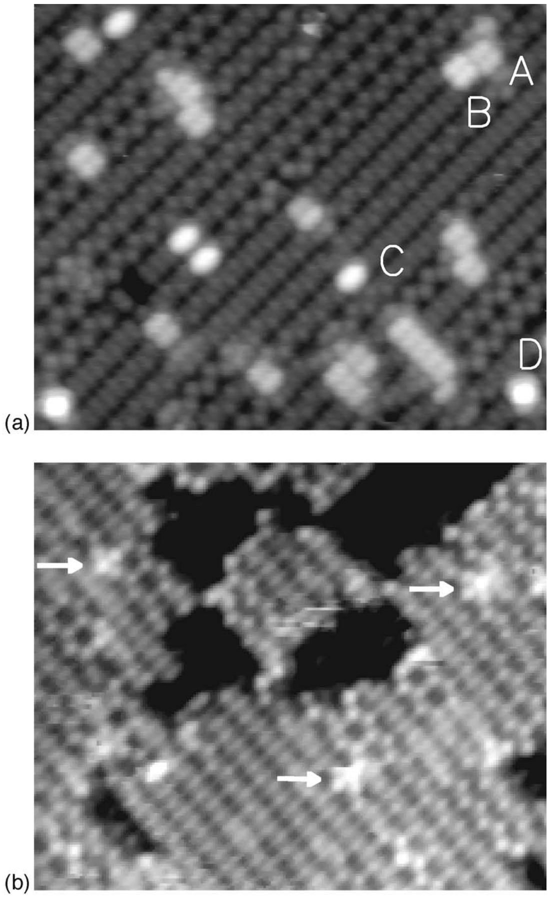

FIG. 1. Experimental STM images of a Ge(001) surface after deposition of 0.1 ML Sb at room temperature (a), and after annealing at 690 K (b). Specific Sb-related features are indicated (see text) (tunneling conditions: $V_{\text{sample}} = -1.9$ V, $I = 1.8$ nA, image sizes 150×125 Å^2).

Oval protrusions elongated perpendicular to the Ge dimer rows, as reported by Chan and Altman,[26] were not observed. After annealing at 690 K, all four types of Sb-related protrusions described above disappear. Pits and Ge islands were created on the surface and characteristic defects [marked by arrows in Fig. 1(b)] appear with low density. Since temperature programmed desorption and auger electron spectroscopy experiments[26] showed that for submonolayer coverages at temperatures lower than 870 K Sb is neither desorbed nor dissolved into the bulk, we assumed that the Sb atoms are either incorporated into the top layer and/or accumulate at step edges on the Ge substrate.

The starting point of our calculations is the clean Ge and Si(001)-$c(2\times4)$ surface terminated with Ge (Si) dimers. The energy of these surfaces is further reduced by dimer buckling, which opens up a Peierls' gap in the initially metallic system. In each dimer one atom is raised and accepts charge from the other atom which moves down below the initially symmetrical position. The relaxed geometries we have ob-

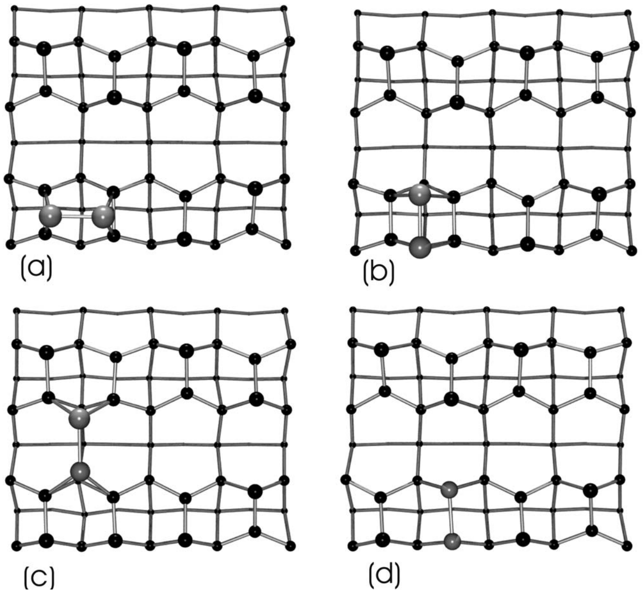

FIG. 2. Schematic atomic structure of the adsorption of Sb_2 on the $c(2\times4)$ reconstruction of Ge(001). Similar configurations were considered for Si(001). The ad-dimer is absorbed (a) orthogonal and on top of Ge (Si) dimers, (b) parallel and on top of Ge (Si) dimers, (c) parallel and in the trenches between Ge (Si) dimers, and (d) substituting a first layer Ge dimer.

tained for the clean Ge(001) and Si(001) surfaces showed the expected $c(2\times4)$ ordering of buckled Ge (Si) dimers. Structural parameters such as the dimer bond length and buckling angle are in good agreement with previous theoretical and experimental results.

A. Adsorption of Sb_2 on Ge(001)

1. Geometry and energetics

We have first studied the adsorption of a single Sb_2 dimer on top of the Ge(001) surface. Three different ways of positioning the Sb dimer on the surface were considered as illustrated in Figs. 2(a)–2(c). Similar configurations were considered for Si(001) and the results are presented in Sec. III D.[35] In geometry 2(a), the ad-dimer is orthogonal to the Si dimers and it is located on top of them.

Geometry 2(b) has Sb dimers parallel to the underlying Ge dimers. In the third configuration, geometry 2(c), the Sb dimer is parallel to the underlying Ge dimers, but it is now in the trenches between two Ge dimer rows. The energies of these arrangements are summarized in Table I. It is found that geometry 2(a) is the configuration that has the lowest total energy for adsorption of Sb dimers on the Ge(001)-$c(2\times4)$ surface. It has no unsaturated dangling bonds: each Ge atom forms bonds with three other Ge atoms and one Sb atom. The Sb atoms are also in a favorable configuration: each Sb atom bonds to two Ge atoms and to another Sb atom, leaving two electrons as a lone pair. Structural parameters are as follows: upon Sb_2 adsorption, the two Ge dimers become almost symmetric, with the Ge–Ge bond length slightly contracted from 2.5 to ~ 2.46 Å. The calculated Ge–Sb and Sb–Sb bond lengths are ~ 2.7 and 2.88 Å respectively. The structural parameters are summarized in Table I. Geometry 2(c) is the stable structure for group III and group IV dimers on Si and Ge(001) surfaces. Although this configuration has been experimentally observed by Chan and Altman,[26] we found that it is energetically very unfavorable, because Sb–Sb, Sb–Ge, and Ge–Ge bonds are highly stretched in this configuration.

Experiments by Chan and Altman[26] and Falkenberg *et al.*[16] have shown that at elevated temperatures Sb dimers start to displace Ge dimers in the top layer. We have examined the possibility that a single Sb dimer displaces a single Ge dimer from the top surface layer [geometry 2(d)]. In this configuration the number of Ge atoms is different from the other cases so a possible way of calculating the energies involved in this process is

$$\Delta E' = E_{\text{Ge-}top} + E_{\text{Sb-}sub} - E_{\text{Sb-}top} - E_{sub}, \qquad (1)$$

where $E_{\text{Ge}-top}$ and $E_{\text{Sb}-top}$ are the total energies of the Ge(001) surface with a single Ge or Sb dimer on top. E_{sub} is the total energy of the Ge(001)-$c(2\times4)$ substrate, and $E_{\text{Sb}-sub}$ is the same as E_{sub} but one of the Ge dimers is re-

TABLE I. Energetics and calculated structural parameters for the adsorption of Sb_4 on Ge and Si(001)-$c(2\times4)$.

	Energy (eV/adatom)	$d_{\text{Sb-Sb}}$ (Å)	$d_{\text{Sb-Ge}}$ (Å)	$d_{\text{Ge-Ge}}$ (Å)
		Sb_2 on Ge(001)		
Geometry 2(a)	0.00	2.88	2.70	2.46
Geometry 2(b)	0.21	2.88	2.75	2.49
Geometry 2(c)	0.50	3.00	2.79	2.50, 2.60
Geometry 2(d)	−0.19	2.88	2.68, 2.71	
		Sb_2 on Si(001)		
Geometry 2(a)	0.00	2.89	2.61, 2.63	2.34
Geometry 2(b)	0.25	2.89	2.67, 2.70	2.36
Geometry 2(c)	0.75	3.01	2.68, 2.70	2.61, 2.37
Geometry 2(d)	0.13	2.90	2.58, 2.60	2.24, 2.28

placed by a Sb dimer. It is found that adsorption of the Sb dimer on top of the first layer is slightly more favorable than adsorption in the second Ge layer by 0.05 eV/adatom. This result shows that it is energetically unfavorable for a Sb dimer to diffuse into the first Ge layer by extracting a single Ge dimer from the Ge(001) substrate. In the experiments, the incorporation of Sb into the top layer occurs after annealing the surface at 520 K, leaving pits and a low density of Ge islands on the surface. Under these circumstances there is an external source of Ge atoms and Eq. (1) does not describe the true conditions for the diffusion of the Sb dimers. A more physical way to compare the energies of the diffused and nondiffused configurations is given by the surface formation energy

$$E' = E_{total} - E_{sub} - N_{\mathrm{Sb}}\mu_{\mathrm{Sb}} - N_{\mathrm{Ge}}\mu_{\mathrm{Ge}}, \qquad (2)$$

where E_{total} is the total energy of the system under consideration, E_{sub} is again the total energy of the Ge(001)-$c(2\times4)$ substrate, $\mu_{\mathrm{Sb}}(\mu_{\mathrm{Ge}})$ is the chemical potential of Sb(Ge) atoms which is taken as the energy of bulk Sb(Ge) atoms in their crystal structure, and $N_{\mathrm{Sb}}(N_{\mathrm{Ge}})$ is the number of Sb(Ge) adatoms in the unit cell. This formula gives an upper limit for the formation energy, since under equilibrium conditions the maximum possible values for μ_{Sb}, and μ_{Ge} are equal to their chemical potential in the bulk phase. Using Eq. (2), it is found that for Sb on Ge(001), a geometry with an embedded Sb dimer in the first Ge layer is more stable by 0.19 eV/adatom as shown in Table I.

2. *Simulated STM images*

To make a direct comparison between our calculated structure and the STM images, we approximate a theoretical tunneling current density $j(\mathbf{r})$ by[36]

$$j(\mathbf{r},V) \propto \int_{E_{F\text{-}eV}}^{E_F} \rho(\mathbf{r},E)dE, \qquad (3)$$

where

$$\rho(\mathbf{r},E) \equiv \sum_{n,\mathbf{k}} |\psi_{n,\mathbf{k}}(\mathbf{r})|^2 \delta(E_{n,\mathbf{k}} - E). \qquad (4)$$

Here $\rho(\mathbf{r},E)$ is the local density of states at the tip position $\mathbf{r}=(x,y,z)$, and the $\psi_{n,\mathbf{k}}(\mathbf{r})$ are the eigenstates of the surface with corresponding energies $E_{n,\mathbf{k}}$.

In Figs. 3(a)–3(c) we show topographic maps of $j(\mathbf{r},V)$=constant at an average distance z $\sim$1 Å above the surface, with $E=-2$ eV for comparison with the experimental STM images with a bias voltage of -2 V (filled states). We observe excellent agreement between theory and experiment [Fig. 3(d)] for Sb dimers orthogonal to the Ge dimers (energetically most stable). The results show that the most prominent protrusions arise from the Sb dimers and, with less intensity (corresponding to lower positions), we observe the atoms of the topmost Ge layer with a $c(2\times4)$ periodicity.

B. Adsorption of Sb_4 on Ge(001)

Chan and Altman[26] have found four basic types of Sb clusters at 320 K. Two of them are the parallel and orthogonal dimers described in the last section. The other two are 3D tetramers and square flat tetramers. The 3D tetramer was observed to change irreversibly into the flat tetramer, while the latter splits to form two separated dimers. Diffusion of both flat tetramers and dimers led to the formation of the (2×1) reconstruction. We have consider six possible arrangements for the adsorption of Sb_4 on Ge(001)-$c(2\times4)$ as shown in Fig. 5 and find that the most stable configuration correspond to the adsorption of Sb_4 as two Sb dimers [geometry 4(f)]. This is in agreement with experiments that observe only dimers after annealing. Structural parameters of both dimers (Table II) are similar to those of a single dimer, indicating that they are noninteracting.

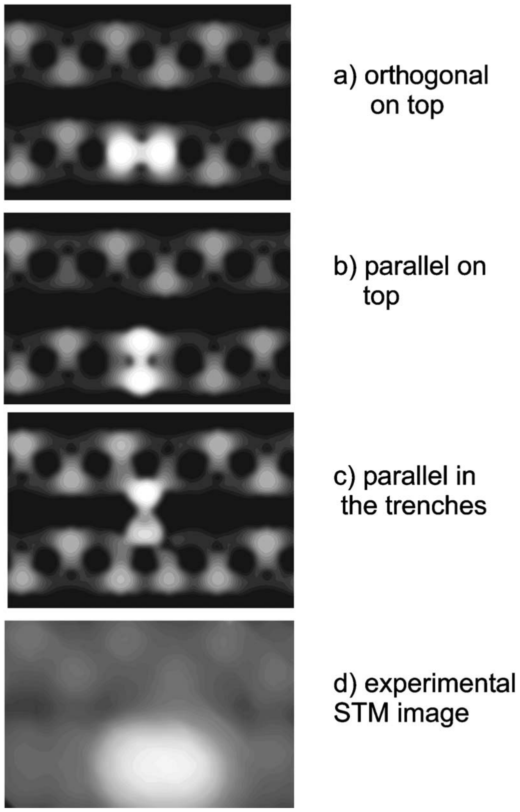

FIG. 3. (a)–(c) Gray-scale plots of the calculated local density of states for Sb_2 on Ge(001)-$c(2\times4)$ for occupied states at E=-2 eV, (d) experimental STM image recorded with $V=-1.9$ V. The image sizes are 24×16 Å^2.

All flat tetramers were found to be more stable than 3D tetramers. This is in agreement with the experimental observation that 3D-tetramers change irreversibly into flat tetramers.

Two different configurations were considered for the adsorption of Sb_4 as 3D clusters. In the first one, shown in geometry 4(a) the molecule is attached to the surface as an inverted pyramid. The Sb atom at the tip of the pyramid forms bonds to the two Ge atoms of a dimer that becomes symmetric. As seen in Table II, this configuration is energetically very unfavorable and it can easily transform into another 3D tetramer as shown in geometry 4(b) Now the Sb_4 molecule is partly broken and it is absorbed on two different dimers. Structural parameters are as follows: upon Sb_4 ad-

TABLE II. Energetics and calculated structural parameters for the adsorption of Sb$_4$ on Ge and Si(001)-$c(2\times4)$.

Sb$_4$ on Ge(001)	Energy (eV/adatom)	$d_{\text{Sb-Sb}}$ (Å)	$d_{\text{Sb-Ge}}$ (Å)	$d_{\text{Ge-Ge}}$ (Å)
		Three dimensional tetramers		
Geometry 4(a)	1.05	Sb1-Sb2∼2.88 Sb2-Sb3∼2.86 Sb2-Sb4∼2.88	Sb1-Ge1∼2.89	Ge1-Ge2∼2.57
Geometry 4(b)	0.32	Sb3-Sb4∼2.89 Sb1-Sb3∼2.85 Sb1-Sb2∼2.84	Sb3-Ge1∼2.66 Sb2-Ge3∼2.67	Ge1-Ge2∼2.47 Ge3-Ge4∼2.46
Flat tetramers				
Geometry 4(c)	0.11	2.90	2.67	2.48
Geometry 4(d)	0.05	2.91	Sb1-Ge1∼2.74 Sb1-Ge5∼2.74 Sb2-Ge3∼2.73 Sb2-Ge6∼2.72 Sb3-Ge1∼2.66 Sb3-Ge2∼2.75 Sb4-Ge3∼2.69 Sb4-Ge4∼2.60	
Geometry 4(e)	0.25	2.92	2.64	
Two dimers				
Geometry 4(f)	0.00	2.88	2.68,2.71	2.46
		Sb$_4$ on Si(001)		
Three dimensional tetramers				
Geometry 4(a)	1.36	Sb1-Sb2∼2.86 Sb2-Sb3∼2.87 Sb2-Sb4∼2.87	Sb1-Si1∼2.72	Si1-Si2∼2.41
Geometry 4(b)	0.5	Sb3-Sb4∼2.89 Sb1-Sb3∼2.84 Sb1-Sb2∼2.83	Sb3-Si1∼2.59 Sb2-Si3∼2.59	Si1-Si2∼2.36 Si3-Si4∼2.34
Flat tetramers				
Geometry 4(c)	0.34	2.90	2.61,2.62	2.38
Geometry 4(d)	0.30	2.91,2.92	Sb1-Si1∼2.67 Sb1-Si5∼2.68 Sb2-Si3∼2.66 Sb2-Si6∼2.66 Sb3-Si1∼2.61 Sb3-Si2∼2.66 Sb4-Si3∼2.62 Sb4-Si4∼2.54	
Geometry 4(e)	0.55	2.88,2.93	2.58,2.67	
Two dimers				
Geometry 4(f)	0.00	2.88	2.61,2.64	2.34

sorption, the two Ge dimers become almost symmetric, with very similar bond lengths: 2.46 and 2.47 Å. Sb$_1$ forms bonds with three other Sb atoms, Sb$_2$ bonds with one Sb and two Ge atoms, while Sb$_3$ and Sb$_4$ bond with two Sb and one Ge atoms. In all cases, each Sb atom is threefold coordinated, and has a lone pair. Bond lengths are given in Table II. To check if this broken Sb$_4$ cluster can be responsible for the ball-shaped protrusions seen in Fig. 1(a) we have simulated STM images for both the inverted pyramid and the broken cluster models. Results are shown in Figs. 4(a) and 4(b)

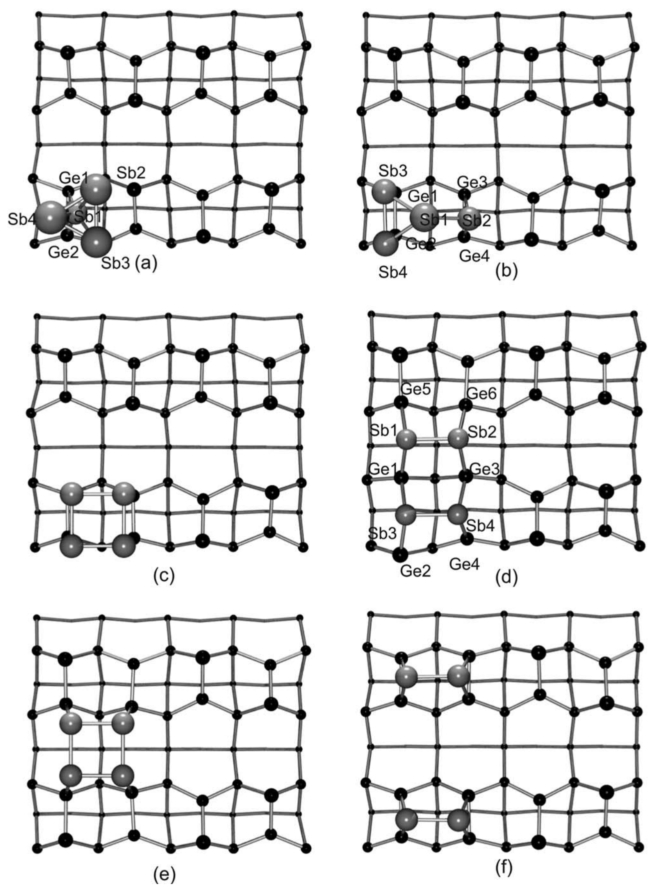

FIG. 4. Schematic atomic structure of the adsorption of Sb_4 on the $c(2\times4)$ reconstructions of Ge and Si(001). (a) 3D cluster as an inverted pyramid, (b) 3D cluster as partially broken pyramid, (c) flat tetramer centered on a dimer row, (d) flat tetramer centered half on a dimer row and half in the trench between dimer rows. (e) flat tetramer centered in between two dimer rows, (f) two dimers.

where we see that both structures yield similar images. Hence from the energetics, we propose that the 3D structure found in the STM images corresponds to the broken Sb_4 cluster model.

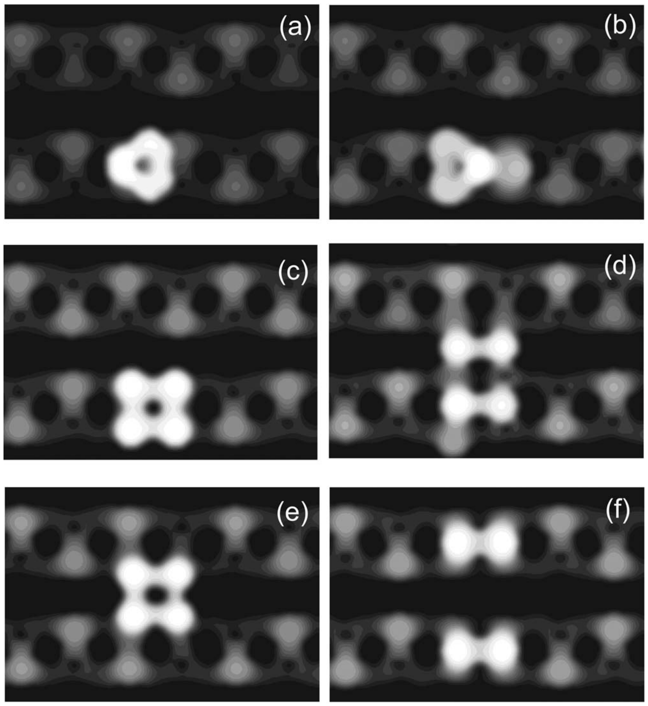

FIG. 5. Gray-scale plots of the calculated local density of states for Sb_4 on Ge(001)-$c(2\times4)$, showing occupied states with $E=-2$ eV. (a) Inverted pyramid, (b) partially broken pyramid, (c) flat tetramer centered on a dimer row, (d) flat tetramer centered half on the dimer row and half in the trench between two dimer rows, (e) flat tetramer centered in the trench between two dimer rows, and (f) two Sb dimers on dimer rows.

Chan and Altman[26] suggested that after Sb arrives on the surface as Sb_4 clusters, they convert to square, flat tetramers. They also found that these clusters reside either centered on top of the Ge dimer row or half on top and half over the trench between dimer rows. In addition we have also observed them centered in between two dimer rows. We have theoretically investigated the adsorption of flat Sb tetramers considering these three possible configurations. After fully relaxing these geometries we found that they correspond to local minima. Geometry 4(c) [Fig. 5(c)] corresponds to the tetramer residing on top of the Ge dimer row. Sb atoms form a square with bond lengths of 2.9 Å, while the length of the Sb–Ge bonds is 2.67 Å. In this arrangement the underlying Ge dimers become symmetric. Geometry 4(e) [Fig. 5(e)] corresponds to the tetramer residing in the trenches between two Ge dimer rows. Sb atoms form a square with bond lengths of 2.91 Å, while the length of the Sb–Ge bonds is 2.65 Å. In this arrangement the Ge dimers remain asymmetric. Geometry 4(d) [Fig. 5(d)] corresponds to the tetramer residing half on top of the Ge dimer row and half over the trough. We found that in this configuration, the Sb tetramer splits into two Sb dimers, but one is located on top of the Ge dimer and the other over the trough. Sb dimer bond lengths are both 2.92 Å, and the underlying Ge dimers are broken. In general the Sb–Ge bonds are not uniform and the structure is asymmetric as shown in Table II and Fig. 5(d). The relative energetics of these flat molecules are in agreement with the results of Chan and Altman; the most stable is geometry 4(d) then geometry 4(c) but they did not observe the least stable geometry 4(e). The simulated scanning tunneling microscopy images are in excellent agreement with the experimental images shown in Fig. 6. Figure 6(a) corresponds to geometry 4(a) or 4(b), Fig. 6(b) corresponds to geometry 4(d) Figure 6(c) corresponds to geometry 4(e) and Fig. 6(d) corresponds to geometry 4(f).

C. Diffusion of flat tetramers on Ge(001)

The different types of cluster can diffuse and modify themselves at room temperature. Geometry 4(c) clusters transform into geometry 4(d) clusters and then into geometry 4(f) clusters. All these processes are reversible. To investigate this aspect further, we have calculated the minimum energy path (MEP). This was obtained by fixing the diffusing dimer laterally at a given position $\mathbf{r}_{\text{parallel}}$ and allowing all other atoms and the height of the dimer to relax. The minima of the MEP give the adsorption sites and the maxima the

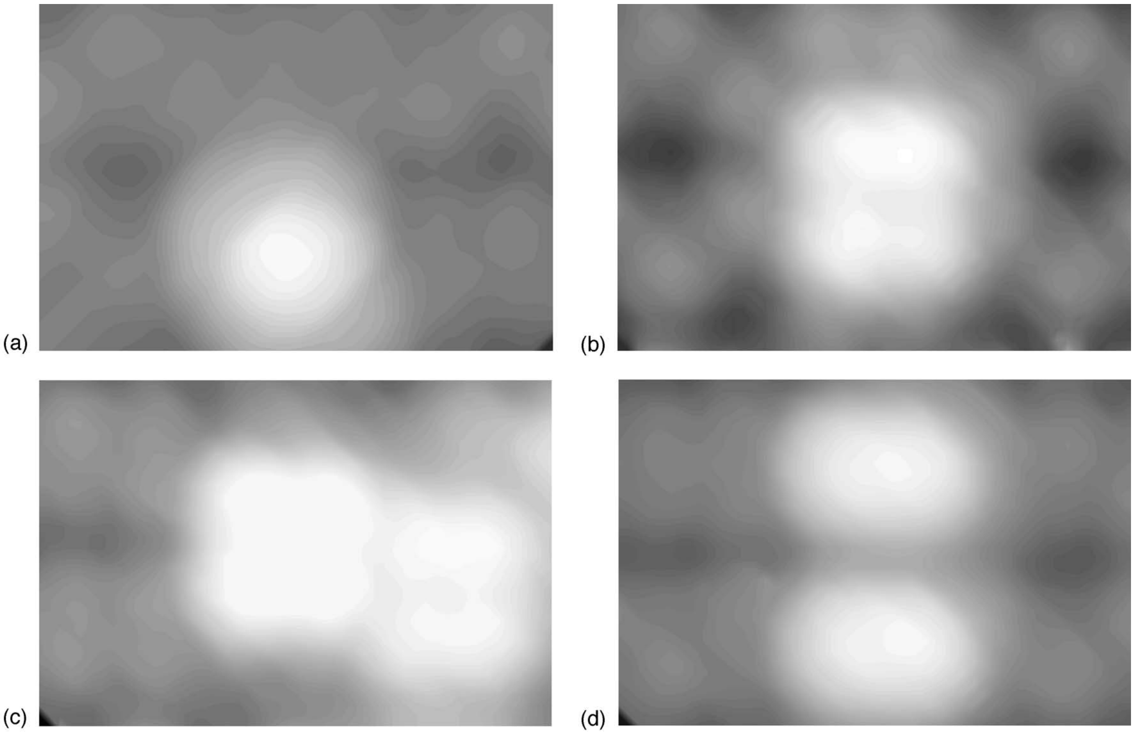

FIG. 6. Experimental STM images showing (a) the ball-shaped protrusion (“D”), (b) a square-shaped protrusion centered half in trenches and half above dimer row (“A”), (c) a square-shaped protrusion centered in the trench between two dimer rows (“B”) next to an “A” type protrusion, (d) two oval protrusions on top of dimer rows (“C”). The images are extracted from Fig. 1(a). The image sizes are 24×16 Å^2.

diffusion barriers. As shown in Fig. 7, the activation energy for the transformation from geometry 4(c) to geometry 4(d) is about 0.3 eV/adatom. There is a small energy gain of 0.05 eV/adatom after the breaking the tetramer. The energy barrier for the transformation from geometry 4(d) to geometry 4(f) is also around 0.6 eV, and there is also a small energy gain of 0.5 eV/adatom for the second dimer to diffuse to a site on top of the Ge dimer rows. The activation barriers for the inverse processes [going from geometry 4(f) to geometry 4(d) and then to geometry 4(c) are ~0.05 eV/adatom larger, hence, it is not surprising that the whole process is reversible as seen in experiment.

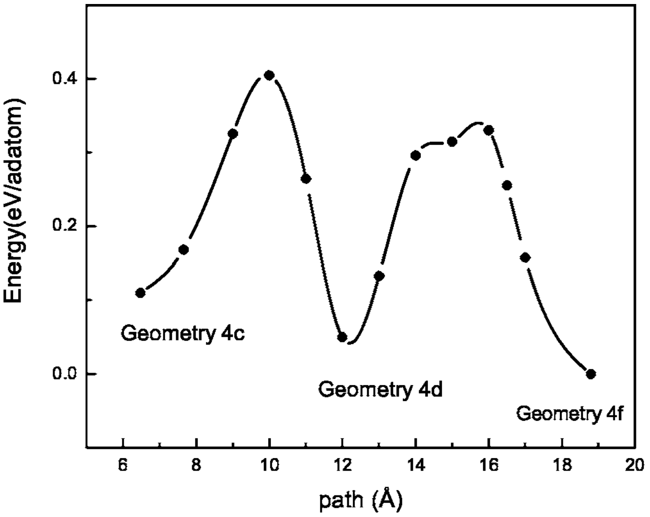

FIG. 7. Energy path for the diffusion of a Sb dimer on the Ge(001) surface.

D. Adsorption of Sb_2 and Sb_4 clusters on Si(001)

For comparison, we have studied the adsorption of Sb_2 and Sb_4 clusters on the Si(001)-$c(2\times4)$ surface. As on the Ge(001) surface, Sb_2 dimers are adsorbed orthogonal to and on top of the underlying Si dimers in the most stable configuration. Structural parameters and energies are summarized in Table I. Several metastable arrangements are found for the adsorption of Sb_4 molecules on the Si(001)-$c(2\times4)$ surface. They can be adsorbed as 3D-clusters or as flat tetramers. The latter are more stable, and can reside either centered on top of the Ge dimer row or half on top and half over the trench between dimer rows, and in the trenches between two dimer rows. However, it is found that it is energetically more favorable for Sb_4 to split into two Sb_2 dimers adsorbed parallel and on top of the Si dimer rows. Energy differences are larger than in the case of Ge(001) so some of the metastable phases may not be present on the Si(001) surface. As shown in Table II, it is not favorable for the Sb_2 dimers to intermix with Si dimers of the first layer, even if there is a source of Si atoms. This is in good agreement with the calculation of Ref. 34.

IV. CONCLUSIONS

First-principles total energy calculations have been performed on the adsorption of Sb_2 and Sb_4 on Ge(001)-$c(2\times4)$ to elucidate the experimental STM images. Similar theoretical results were found for the adsorption of Sb on Si(001)-$c(2\times4)$ surfaces. We found that it is energetically more favorable for Sb_4 to split into two Sb_2 dimers each adsorbed parallel and on top of the Ge (Si) dimer rows. However, several other metastable configurations may coexist. Our simulated STM images are in excellent agreement with the experimental results. We also investigated the diffusion of the dimers into the first Ge (Si) layer theoretically and found that it is favorable for the Sb_2 dimers to intermix with Ge dimers in the first layer if there is a source of Ge atoms. In the case of Si(001) surfaces intermixing with Sb dimers is unfavorable.

ACKNOWLEDGMENTS

Calculations were carried out at the supercomputer center of DGSCA-UNAM. We acknowledge support from DGAPA-UNAM Project # IN101103. We thank C. González for technical support.

---

[1] M. Copel, M. C. Reuter, E. Kaxiras, and R. M. Tromp, Phys. Rev. Lett. **63**, 632 (1989).

[2] M. Horn-von Hoegen, M. Copel, J. C. Tsang, M. C. Reuter, and R. M. Tromp, Phys. Rev. B **50**, 10811 (1994).

[3] M. Richter, J. C. Woicik, J. Nogami, P. Pianetta, K. E. Miyano, A. A. Baski, T. Kendelewicz, C. E. Bouldin, W. E. Spicer, C. F. Quate, and I. Lindau, Phys. Rev. Lett. **65**, 3417 (1990).

[4] S. Tang and A. J. Freeman, Phys. Rev. B **47**, 1460 (1993).

[5] J.-H. Cho and M.-H. Kang, Phys. Rev. B **51**, 5058 (1995).

[6] S. J. Jenkins and G. P. Srivastava, Surf. Sci. **352–354**, 411 (1996).

[7] N. Takeuchi, Phys. Rev. B **55**, 2417 (1997).

[8] S. J. Jenkins and G. P. Srivastava, Phys. Rev. B **56**, 9221 (1997).

[9] D. H. Rich, T. Miller, and T. C. Chiang, Phys. Rev. B **41**, 3004 (1990).

[10] M. C. Hakansson, U. O. Karlsson, J. Kanski, P. O. Nilsson, Y. Khazmi, and K. Hricovini, Surf. Sci. **278**, L131 (1992).

[11] M. Lohmeier, H. A. van der Vegt, R. G. Van Silfhout, E. Vlieg, J. M. C. Thornton, J. E. Macdonald, and P. M. L. O. Scholte, Surf. Sci. **275**, 190 (1992).

[12] A. Lessmann, W. Drube, and G. Materlik, Surf. Sci. **323**, 109 (1995).

[13] D. H. Rich, F. M. Leibsle, A. Samsavar, E. S. Hirschorn, T. Miller, and T. C. Chiang, Phys. Rev. B **39**, 12 758 (1989).

[14] D. H. Rich, T. Miller, G. E. Franklin, and T. C. Chiang, Phys. Rev. B **39**, 1438 (1989).

[15] D. H. Rich, G. E. Franklin, F. M. Leibsle, T. Miller, and T. C. Chiang, Phys. Rev. B **40**, 11804 (1989).

[16] G. Falkenberg, L. Seehofer, and R. L. Johnson, Surf. Sci. **377**, 75 (1997).

[17] J. Nogami, A. A. Baski, and C. F. Quate, Appl. Phys. Lett. **65**, 475 (1991).

[18] H. B. Elswijk and E. J. v. Loenen, Ultramicroscopy **42-44**, 884 (1992).

[19] B. Garni, I. L. Kravchenko, and C. T. Salling, Surf. Sci. **423**, 43 (1999).

[20] Y. W. Mo, Phys. Rev. Lett. **69**, 3643 (1992).

[21] Y. W. Mo, Phys. Rev. B **48**, 17 233 (1993).

[22] Y. W. Mo, Phys. Rev. Lett. **71**, 2923 (1993).

[23] Y. W. Mo, J. Vac. Sci. Technol. B **12**, 2231 (1994).

[24] S. Rogge, R. H. Timmerman, P. M. L. O. Scholte, L. J. Geerligs, and H. W. M. Salemink, Phys. Rev. B **62**, 15341 (2000).

[25] M. A. Boshart, A. A. Bailes III, A. Dygo, and L. E. Seiberling, J. Vac. Sci. Technol. A **13**, 2764 (1995).

[26] L. H. Chan and E. I. Altman, Phys. Rev. B **63**, 195309 (2001).

[27] R. J. Dixon, C. F. McConville, S. J. Jenkins, and G. P. Srivastava, Phys. Rev. B **57**, R12701 (1998).

[28] R. Car and M. Parrinello, Phys. Rev. Lett. **55**, 2471 (1985).

[29] P. Hohenberg and W. Kohn, Phys. Rev. **136**, B864 (1964).

[30] W. Kohn and L. J. Sham, Phys. Rev. **140**, A1133 (1965).

[31] N. Takeuchi, Phys. Rev. B **56**, 7446 (1997).

[32] L. Kleinman and D. M. Bylander, Phys. Rev. Lett. **48**, 1425 (1982).

[33] N. Takeuchi, J. Vac. Sci. Technol. A **16**, 1790 (1998).

[34] N. Takeuchi, J. Vac. Sci. Technol. A **14**, 1652 (1996).

[35] M. Ramamoorthy, E. L. Briggs, and J. Bernholc, Phys. Rev. Lett. **81**, 1642 (1998).

[36] A. Selloni, P. Carnevalli, E. Tosatti, and C. D. Chen, Phys. Rev. B **31**, 2602 (1985).